Toxicology Methods, 11:107–126, 2001

1051-7235/01 $12.00 + .00

GAS MICROBUBBLES IN BIOLOGY: THEIR RELEVANCE IN HISTOLOGY, TOXICOLOGY, PHYSIOLOGY, AND ANESTHESIA

Donald R. VanDeripe
Mallinckrodt Medical, St. Louis, Missouri, USA

Pilot studies in 31 rats to detect gases in the brain during anesthesia demonstrated the presence of gas microbubbles in electron photomicrographs of brains taken from anesthetized and unanesthetized control animals. Gas microbubbles were numerous in specimens preserved with near-isotonic fixatives, but nearly absent in brains fixed with a substantially hypertonic fixative solution. Hypertonic fixation appears to deplete extracellular and intracellular fluid to an extent that tissue entrapped bubbles collapse and are flushed away. Using near-isotonic fixative solutions, it was shown that gas microbubbles may play important roles in Toxicology (CCl4-induced hepatotoxicity), Physiology (oxygen transport), and Pharmacology (inhalation anesthesia). Excessively hypertonic tissue fixative solutions are unsuitable for the histological study of tissue gases.

Keywords anesthetic mechanisms, CCl4-induced hepatotoxicity, electron microscopy, gas microbubbles, oxygen transport, vapor pressures

Initially, the purpose of this study was merely to determine whether microbubbles of gas could be found in the brains of rats anesthetized with gas and volatile anesthetics. The premise was that anesthetic gas bubbles might interfere with normal brain function by simple physical mechanisms. A pilot study, conducted on rats anesthetized with methoxyflurane, halothane, ethyl ether, or nitrous oxide, confirmed the presence of gas microbubbles in brains fixed in 2% glutaraldehyde. Surprised to find gas bubbles in the brain of an unanesthetized control rat, the author reviewed earlier literature to determine which fixatives were optimum for rat brains. In 1969, Sumi found that mitochondria were swollen and vacuolated and the neuroprocesses were swollen in 24-h-old ether-anesthetized rats perfused with 50 to 100 mL of 1.2% glutaraldehyde buffered to 280 mOsm/kg (isotonic). These findings were attributed to poor tissue fixation, since they disappeared in rats perfused with 50 to 100 mL of 4% glutaraldehyde buffered to 710 mOsm/kg (~2.5 ×

Received 15 May 1999; accepted 25 October 2000.
Address correspondence to Dr. D. R. VanDeripe, 1534 Woodbury Drive, St. Charles, MO 63304.

hypertonic). Whereas Sumi's large-volume hypertonic fixation provided superior electron microscopy (EM) pictures, it suggested to this author the potential for an osmotic reduction in tissue water, which could be expected to flush out tissue-entrapped gas microbubbles. Therefore, the bubbles might be real, not artifact. The pilot study was then extended to determine whether near-isotonic fixation was consistent with more tissue bubbles than was hypertonic fixation. These studies are reported in four parts, with separate results, discussions, and conclusions.

MATERIALS AND METHODS

Materials

The materials used were methoxyflurane (Pitman Moore, Mundelein, IL), ethyl ether (Mallinckrodt, St. Louis, MO), enflurane (Abbott Park, IL), isoflurane (Ohmeda Liberty Corner, NJ), nitrous oxide (Union Carbide, Danbury, CT), xenon (Air Products, Allentown, PA), halothane, flurothyl, pentane, octane, and decane (Aldrich, Milwaukee, WI). Glutaraldehyde was EM grade (Sigma Chemical, St. Louis, MO) diluted with water for injection (Abbott). The study used 31 female Sprague–Dawley rats (200–325 g).

Methods

All procedures were conducted at ambient laboratory temperature of approximately 25°C. An 8-L stainless steel cylinder fitted with an elevated wire mesh shelf and a clear glass cover served as the anesthesia chamber. Volatile anesthetics (1–5 mL) were poured onto gauze pads on the floor of the cylinder, and flowing gases were layered-in just below the wire shelf. When deep anesthesia (slowed respiration, loss of righting reflex, absent paw-pinch pain reflex) was achieved, the rats were removed from the chamber and immediately sacrificed via guillotine or systemic vascular perfusion. Perfusions were accomplished using 7 mL of the fixative injected manually at 1 mL/s via syringe with a catheter tip positioned in the left ventricle at the aortic valve. Three rats were perfused for longer times with 30 to 50 mL of fixative solution. Following perfusion or decapitation, rat brains were immediately removed from the skulls and immersed in 15 mL of the fixative contained in a 30-mL amber bottle. Processing of the samples for EM included postfixation with 1% osmium tetroxide, dehydration in graded ethanol, embedding in Spurr's resin, and slicing into ultramicrotome thin sections. Samples of cerebral cortex gray and white matter were viewed and photographs taken on a JEOL 100CX transmission electron microscope. Negatives were

TABLE 1. Gas Bubbles in Brain Electron Photomicrographs

Agent (Number of rats)	Anesthetic time (min)	Fixative[a]	Gray matter			White matter		
			n	Mean	SD	*n*	Mean	SD
Methoxyflurane (1)	4	2G	5	1856+	141	5	440+	266
Ethyl ether (1)	10	2G	5	824+	245	5	479+	103
Halothane (3)	3	2G	18	751+	257	8	511+	59
Halothane (1)	2	3G	6	601+	94	3	592+	20
Isoflurane (3)	5	3G	21	487+	116	16	420+	57
Nitrous oxide (1)	1	2G	5	718+	129	3	179	59
Enflurane (2)	9	3G	12	492+	132	12	323+	41
Pentane (1)[b]	6	3G	6	516+	75	6	254	52
Flurothyl (1)	8	3G	6	315*	42	6	390+	41
Xenon (2)	2	3G	12	315	188	12	287	10
Control (2)	U	2G	11	400	96	8	208	101
Octane (1)[c]	U	3G	3	240*	47	3	194	57
Decane (1)[c]	U	3G	3	232*	73	3	279	86
Ethyl ether (1)	NR	BF	6	62*^	17	6	45*^	11
Ethyl ether (1)[d]	NR	BF	6	70*^	3	6	110*^	11
Ethyl ether (2)[e]	NR	BF	12	143*^	57	12	169*^	38

Note. *n*, number of pictures (each 460 sq cm) counted for total bubble numbers; NR, not recorded; SD, standard deviation; U, unanesthetized; +, more; *, fewer bubbles than gray or white matter controls, $p < .05$. ^, fewer bubbles than ether rat perfused with 2G, $p < .001$.

[a] 2G, 2% glutaraldehyde; 3G, 3% glutaraldehyde; all were perfused with 7 mL except the unanesthetized (guillotined) rats.

[b] 50 mL added to anesthetic chamber.

[c] 50 mL added to anesthetic chamber, but no anesthesia during a 15-min exposure.

[d] 50 mL saline followed by 30 mL BF.

[e] 50 mL BF; BF, 7.47× hypertonic buffered fixative.

prepared at magnifications of ×6000, ×24,900, ×48,000, and ×78,000 and printed as 7.5″ × 9.5″ (460 sq cm) fields on 8″ × 10″ photographic paper. Total bubbles per photograph were counted through a transparent grid for all ×6000 pictures. Criteria for a gas bubble were that the structure be circular to ovoid in shape and transparent in appearance. Statistical evaluations (Student's *t*-test) were conducted mainly to assess potential trends of the data in Table I. The experimental protocols in this report were approved by the Mallinckrodt Medical Inc. animal use committee.

Histology

In the study, 7 rats (5 anesthetized rats and 2 controls) were killed via guillotine, and their brains were removed and quartered. Each quadrant was immediately immersed in 1 of 4 different fixatives: 2% glutaraldehyde (2G); 3% glutaraldehyde (3G); 6% glutaraldehyde (6G); or a hypertonic buffered fixative (BF) having the following formulation:

TABLE 2. Picture Bubble Counts in Rat Brain Quadrants vs. Fixative Solution Tonicity

Agent (Number of rats)	*n*	2G	3G	6G	BF
Control (2)	8	289	221	266	41*
Nitrous oxide (1)	4	371	272	259	83*
Halothane (4)	16	288	408	336	137*

Note. *n*, number of ×6000 pictures counted for total bubbles at each fixative concentration; 2G, 2% glutaraldehyde; 3G, 3% glutaraldehyde; 6G, 6% glutaraldehyde; BF, 7.47× hypertonic buffered fixative; *, fewer bubbles than treatment-respective glutaraldehyde fixative solutions, $p < .01$.

BF ingredient:	Tonicity vs. 0.9% NaCl:
2% Glutaraldehyde	0.65×
3% Paraformaldehyde	3.25×
NaH_2PO_4 (16.48 g/L)	1.80×
KH_2PO_4 (4.90 g/L)	0.47×
NaCl (11.68 g/L)	1.30×
Total	7.47×

These fixatives solutions were calculated to be 0.65× (2G), 1.0× (3G), 2.0× (6G), and 7.47× (BF) the tonicity of a 0.9% solution of NaCl, respectively. Treatment groups included 2 controls, 1 nitrous oxide rat, 4 halothane rats. The total number of ×6000 pictures counted for bubbles were as follows: controls, 32; nitrous oxide rats, 16; and halothane rats, 64. See Table 2 for data.

Five ether-anesthetized rats were perfused as detailed previously: 1 with 7 mL of 2G; 1 with 7 mL of BF; 1 with 50 mL of saline followed by 30 mL of BF; and 2 with 50 mL of BF. The total number of pictures counted for bubbles were as follows: 2G ether rats, 10; 4 BF ether rats, 12 each—that is, 48 pictures in all. See Figure 1 and Table 1 for data.

Toxicology

No experiments were done. The information is taken from an article in the literature. (See the "Toxicology" section and Figure 2.)

Physiology

The pictures in Figure 3 were selected from data listed in Table 1: the 2G decapitated controls, the 2G halothane rats, and the 2G nitrous oxide rats. The picture in Figure 4 was selected from the 5 × 24,900 magnification prints available for the initial 2G control rat.

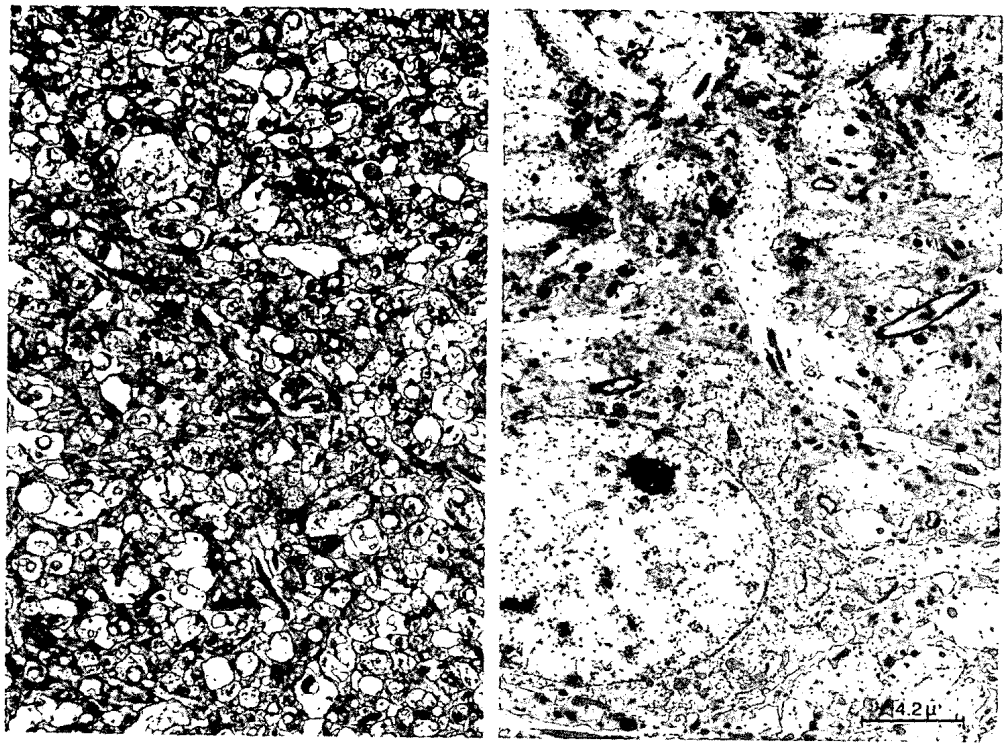

(A) (B)

FIGURE 1. Identical brain perfusions of rats under ether anesthesia using different fixative solutions. Each ×6000 panel equals 230 sq cm. (A) Rat brain gray matter perfused with 7 mL 2% glutaraldehyde as the fixative. (B) rat brain gray matter perfused with 7 mL 7.47× hypertonic buffered fixative. (A) is full of transparent bubbles, whereas (B) is nearly devoid of bubbles. μ, μm (micron).

Anesthesia

In this segment, 24 rats were treated as follows: perfused with 2G, 6; perfused with 3G, 10; perfused with BF, 4; decapitated 2G, 2; and decapitated 3G, 2. See Table 1 for detailed information. The total number of ×6000 pictures (n) counted for bubbles in Table 1 was 251. It is to be noted that 5 of these rats were also included in the "Histology" section.

GAS MICROBUBBLES IN HISTOLOGY

Results

The first experiment was an internally controlled study wherein 5 anesthetized rats and 2 controls were decapitated, their brains quickly removed and quartered, and each sample immersed in 1 of the 4 fixatives listed in the "Methods" section. Bubble counts in these picture clearly indicate a loss of bubbles in the segments immersed in the BF (Table 2).

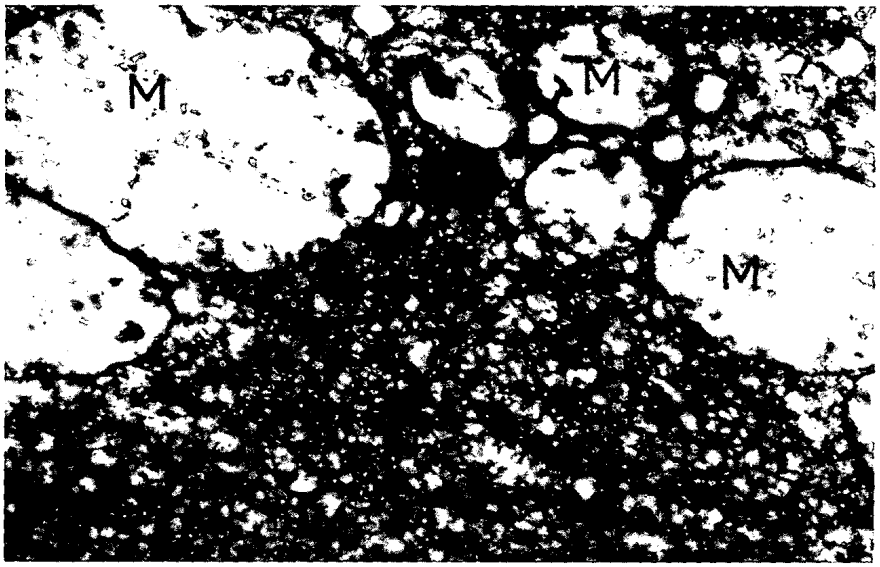

(A)

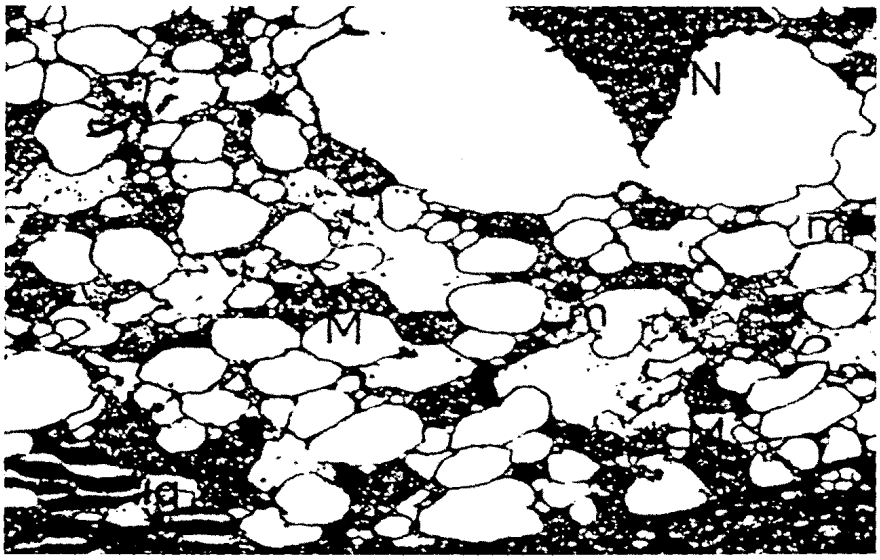

(B)

FIGURE 2. Electron photomicrographs of CCl_4-induced hepatotoxicity in rats. (A) Rat sacrificed 2 h after intoxication with carbon tetrachloride. Degeneration of mitochondria (M), which are swollen, may be seen. The cristae are very rare. The matrix is replaced by fleecy filaments. The hyaloplasm is composed of microvesicles and filaments. (B) Rat sacrificed 12 h after the injection of carbon tetrachloride. Part of a cell in the form of a *ballon*. The cytoplasm is composed of large vacuoles between which persist the mitochondria (M) and the microcorpuscles (m). In the upper right, the nucleus (N) is small and dense. ig, fatty inclusions. (Oberling and Rouiller 1956). © Masson Editeur, Paris 1956.

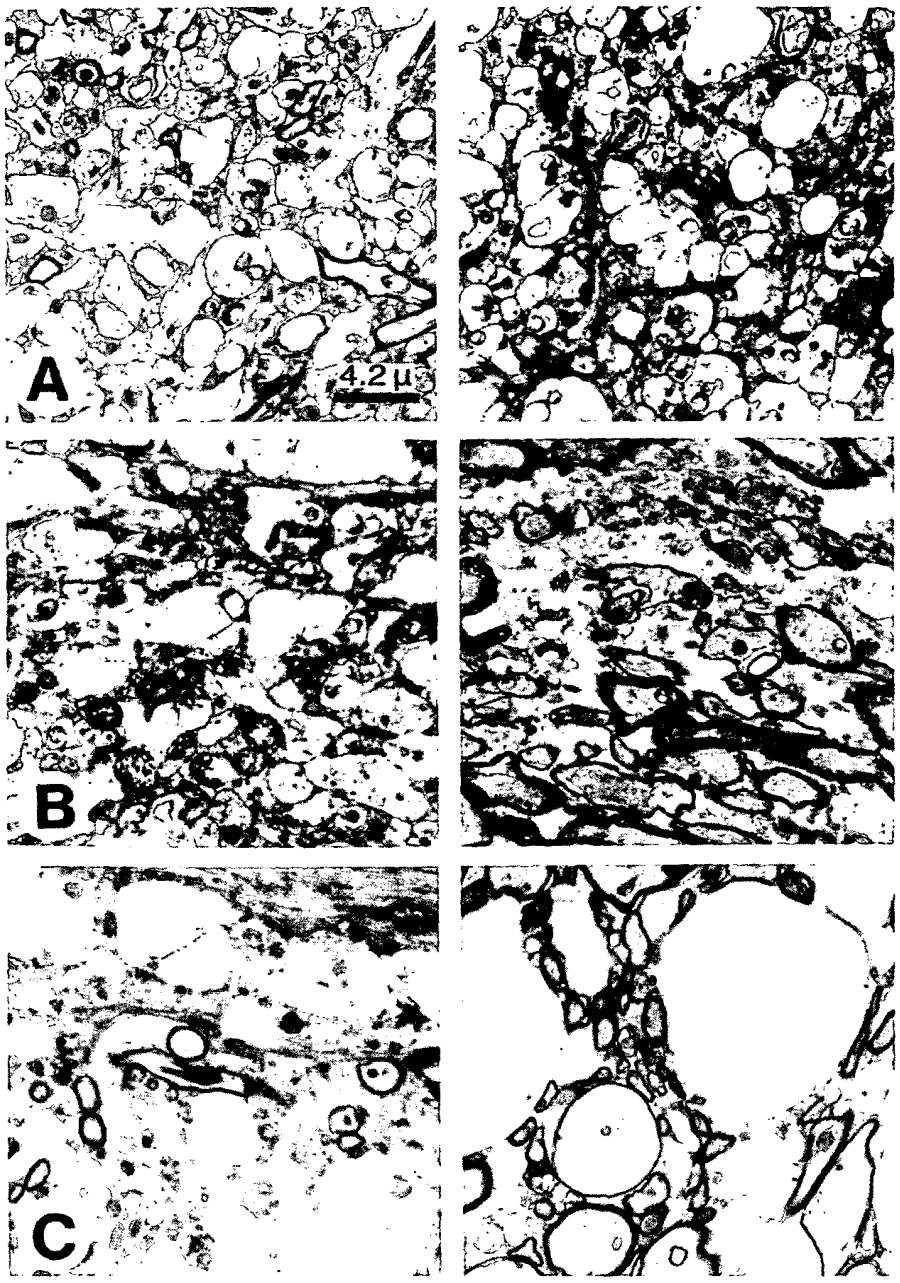

FIGURE 3. Electron photomicrographs of rat brains ×6000. Size, 1/8 the original 7.5″ × 9.5″ (57 sq cm). Fixative solution, 2% glutaraldehyde. (A) Halothane-affected rat brain gray matter; halothane-affected rat brain white matter. Note the large number of transparent gas bubbles. (B) Control rat brain gray matter; control rat brain white matter. (C) Nitrous oxide–affected rat brain gray matter; nitrous oxide–affected rat brain white matter. Note the larger gas bubbles. μ, μm (micron).

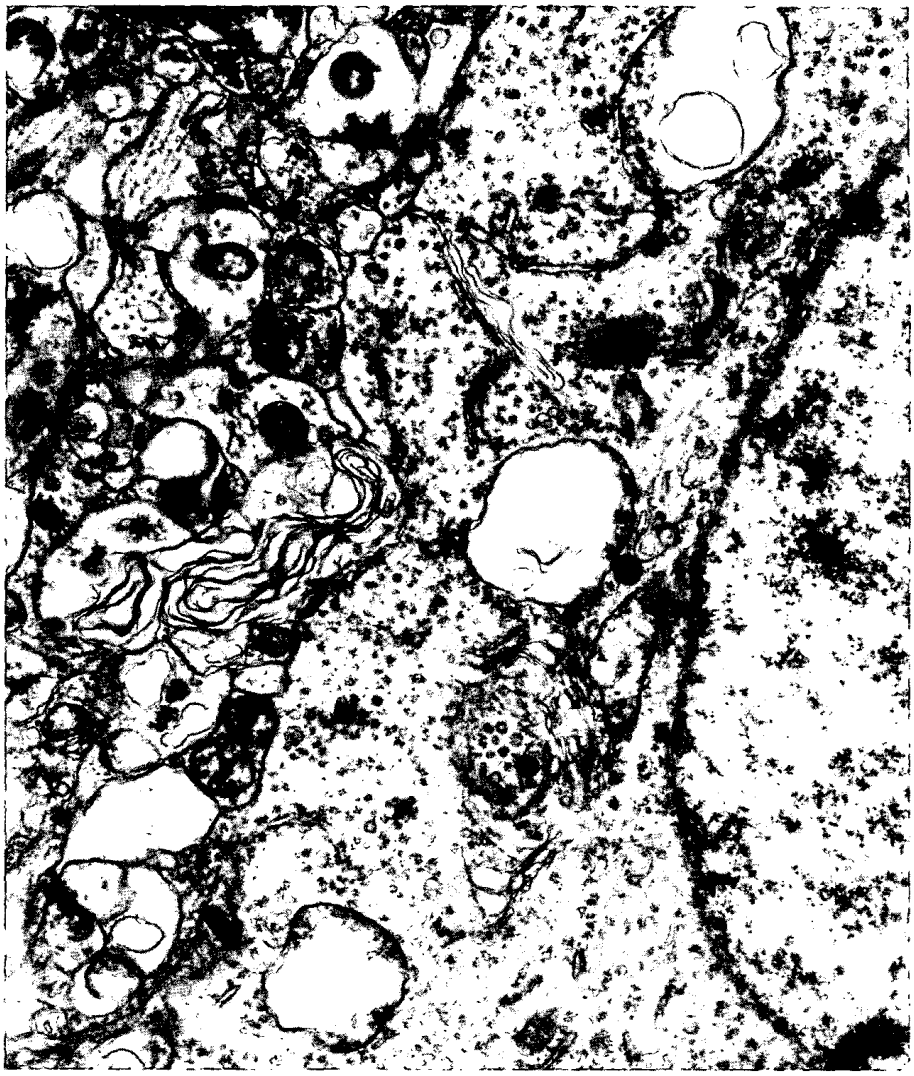

FIGURE 4. Control rat brain gray matter ×24,900. Fixative solution, 2% glutaraldehyde. Three gas-filled mitochondria. Top right, two remnants of bubble "shells" may be seen; center, bubble uptake is in progress; bottom left, a compliant mitochondrial membrane. As an untreated control, the gas must be oxygen and/or nitrogen.

The second experiment compared the number of bubbles seen in the ether-anesthetized rat perfused with 7 mL of 2G with the number of bubbles seen in the ether-anesthetized rat perfused with 7 mL of BF. Gray matter pictures in these rats clearly depict numerous bubbles in the 2G brain and the absence of bubbles in the BF brain (see Figure 1). Bubbles numbers in the pictures, tabulated in Table 1, clearly indicate a dramatic reduction of bubble numbers in the rat perfused with 7 mL of BF compared to those in the rat perfused with 7 mL of 2G. As well,

3 rats perfused with 30 to 50 mL of BF showed similar reductions in total bubble counts (Table 1).

Discussion

Two conflicting issues emerge when one considers tissue fixation in histology. The first issue is that photomicrographs of tissue specimens fixed in isotonic fixatives appear as swollen, with vacuoles and swollen mitochondria, and appear to be poorly fixed and "noisy." The second issue is that tissue specimens fixed in nonphysiological, hypertonic fixatives provide highly detailed, histologically informative pictures. Which of these two approaches is correct?

Sumi noted swollen and vacuolated mitochondria and swollen neuronal processes in 24-h-old ether-anesthetized rats perfused with 50 to 100 mL of a 1.4% glutaraldehyde buffered to 280 mOsm/kg (isotonic) and considered these swellings to be abnormal and to effectively fill the extracellular space. Conversely, pictures of 24-h-old ether-anesthetized rats perfused with equal volumes of a 4% glutaraldehyde solution buffered to 710 mOsm/kg (~2.5× hypertonic) demonstrated a greater extracellular space and no swelling of mitochondria and was therefore preferred to the isotonic fixative solution. That Sumi's isotonic fixative may have demonstrated swelling and vacuolization of the mitochondria due to the retention of physiological gases (oxygen and nitrogen) or vapors of the ether anesthetic was not considered. Conversely, high-volume perfusion with hypertonic fixatives might be expected to deplete enough tissue fluids to cause the collapse and washout of entrapped gas bubbles and thereby minimize tissue gas microbubble noise. Indeed, Sumi's EM photomicrographs of brains perfused with the 2.5× hypertonic fixative show many dense and crenated (gas-depleted) mitochondria and dense cellular matrix. There must come a point when tissues perfused with hypertonic fixatives lose significant quantities of water to the perfusion fluid. Gonzales-Aguilar (1969) used 12M (20× hypertonic) formaldehyde for perfusion of rat brains and noted visible dehydration of the brains perfused for 15 min. He reported, "A coarse shrinkage of the nervous tissue was evident upon opening the skull. Indeed, the brain looked like a walnut within its shell." Perfusion with this fixative for only 60 s produced a loss of water from the brain amounting to at least 4% of its weight.

Ascribing EM photomicrograph transparencies (swellings and vacuoles) to be artifacts of tissue fixation does not allow for the presence of gas bubbles in tissue specimens. However, based on boiling points and vapor pressures, many substances (including molecular oxygen) are obligate gases at body temperature, and near-isotonic tissue fixation

provides for the study of these tissue gas deposits. Conversely, substantially hypertonic tissue fixation expels tissue gases (noise) and enhances micro-anatomic detail.

Conclusions

Notwithstanding the descriptive term used—swelling, vacuole, inclusion body, artifact, etc.—it is the author's contention that any structure transparent to the EM beam must be gaseous. Earlier literature and the results of these pilot experiments mentioned clearly demonstrate that tissue fixation with substantially hypertonic fluids depletes tissue water causing a collapse (loss) of entrapped gas bubbles. Compared to near-isotonic tissue fixation, hypertonic fixatives are unsuitable for monitoring tissue gas deposits in toxicolgy, physiology, and anesthesia (pharmacology) as is reported below.

GAS MICROBUBBLES IN TOXICOLOGY

Results

Oberling and Rouiller (1956) administered carbon tetrachloride (CCl_4) by intraperitonal injection at a dose of 600 mg/kg to a number of rats and studied the EM-detected liver changes over a period of 11 days. As soon as 2 h after the injection, livers fixed in a buffered 1% osmium tetroxide solution began to show the presence of vacuoles and mitochondrial swelling, which was more impressive at 12 h and persisted after 48 h when tissue necrosis ensued. Notable observations, described in the legends of their 19 EM figures included cells "en ballon," gaint transparent vacuoles, degenerated swollen mitochondria, and clear swollen mitochondria. Figure 2A shows transparent swollen mitochondria described as degenerated with very few cristae in a rat sacrificed 2 h after administration of CCl_4. At 12 h (Figure 2B), large transparent vacuoles dominate the tissue section.

Discussion

Because CCl_4 is a volatile solvent with vapor pressure properties not too dissimilar, from those of volatile anesthetics, the author searched the CCl_4 literature for articles that featured EM methodology and photomicrographs. The Oberling and Rouiller article provided several EM photomicrographs that documented swollen, transparent mitochondria and tissue vacuolization. Could the presence of CCl_4 as a gas shed some light on the mechanism of its hepatotoxicity? The key descriptive terms used by Oberling and Rouiller are the words "clear" and "transparent,"

TABLE 3. Physical Properties and Activities of Anesthetics

Agent	Boiling point (°C)	Vapor pressure (mmHg/°C)	Water solubility (%)	Anesthetic activity
Decane	174			Inactive
Octane	125.6		Insoluble	Inactive
Methoxyflurane	105	22.5/20*		Potent
Flurothyl	63.9		Insoluble	Convulsant
Enflurane	56.5	175/20*		Clinical
Halothane	50.2	243/20*		Clinical
Isoflurane	48.5	250/20*		Clinical
Body temperature: 37°C				
Pentane	36.1			Weak
Ethyl ether	34.6	440/20*	6	Clinical
Cyclopropane[a]	−33		~37	Clinical
Nitrous oxide	−88		~50	Clinical
Xenon	−108		~11	Weak

Note. All data from *Merck Index*, 12th ed. 1996, except * from Goodman and Gilman's *The Pharmacologic Basis of Therapeutics*, 8th ed. 286, 1990.

[a]Not studied.

which describe liver specimens ladened with gas. Since CCl_4 boils at 76.2°C, not far from the boiling point of volatile anesthetics (Table 3), it must equilibrate into liquid and gas phases in vivo at body temperature (Rogers and Hill 1978). Vaporizing at a rate faster than the rate of its pulmonary clearance would result in an accumulation of gaseous CCl_4 in the hepatic parenchyma, where it could fill mitochondria and accumulate as transparent vacuoles, as is shown in Figure 2A and B.

Mitochondria full of the inert CCl_4 gas might be unable to take up oxygen, which would lead to shutdown of aerobic metabolism, a shift to anaerobic metabolism, acidosis, cell death and, eventually, tissue necrosis. Interestingly because, volatility is temperature-dependent, lowering the body temperature might slow the vaporization of CCl_4 to a point where its hepatotoxic effects could be delayed. This, in fact, has already been well documented. Larson and Plaa (1965) observed that lowering the body temperature of rats by transection of the spinal cord delayed the onset of CCl_4-induced hepatotoxicity, and similar protective measures were subsequently reported following drug-induced hypothermia from chlorpromazine (Marzi et al. 1980), trifluperazine (Villarreul et al. 1986), and phenylmethylsulfonyl fluoride (deFerreyra et al. 1989).

Conclusions

It seems likely that the toxicity of carbon tetrachloride to the hepatic mitochondria is mediated in the form of CCl_4 gas vapors that fill mitochondria to capacity, thereby blocking further uptake of oxygen. In turn, this leads to anaerobic metabolism, acidosis, cell death, and tissue necrosis.

The protective effect of hypothermia probably results from a decrease in the volatility of CCl_4. In a broader sense, such findings suggests a toxic potential for any chemical that develops a significant gas-forming vapor pressure at body temperature.

GAS MICROBUBBLES IN PHYSIOLOGY

Results

Gas microbubbles were seen in decapitated control and unanesthetized (octane and decane) rat brains (Figure 3B, Tables 1 and 2). Gases that could logically account for bubbles in these unanesthetized animals would be physiological microsuspensions of oxygen, nitrogen, and carbon dioxide, the last being least likely because it has a high affinity for deoxyhemoglobin and can also be buffered out as bicarbonate. Both intermediate in solubility, oxygen (3%) and nitrogen (1.5%) would be expected to form bubbles larger than those in most of the volatile anesthetics, but smaller than those in the highly soluble gases nitrous oxide and xenon, and this appears to be the case (Table 3; Figure 3B and C). In Figure 4, one is struck by 3 swollen mitochondria in a picture of a control rat. These highly magnified mitochondria must be full of oxygen or nitrogen, not anesthetic. The mitochondrion at the top shows residual evidence of 2 membranes of recently engulfed gas bubbles; the mitochondrion in the middle shows bubble uptake in progress; and the mitochondrion at the bottom demonstrates pliancy of the mitochondrial membrane. This picture and most of those in Figure 5 show cristae pushed toward the outer wall as the mitochondria fill with gases.

Discussion

Again, the operative word in describing these mitochondria is "transparent," which mandates that they be gas-filled, not swollen with liquid. Gas bubbles taken into mitochondria could, in part, be oxygen bubbles and may represent a mechanism by which oxygen can accumulate as an intramitochondrial store for use in oxidative metabolism. This makes sense when one approximates some basic calculations: (1) brain weight (1.4 kg) × brain water (80%) = 1120 mL of brain water; (2) oxygen solubility (3%) ×1120 mL of water = 33.6 mL as brain water oxygen capacity; (3) cardiac output (5L) × brain fraction (10%) = 500 mL/min of brain blood flow; (4) blood oxygen arteriovenous difference (19.5 – 13.5 = 6 mL/100 mL of blood; (5) 6 mL × 500 mL/min = 30 mL of oxygen delivery to the brain per minute. Thus, (2) (33.6 mL oxygen capacity of brain water) and (5) (30 mL/min oxygen deliver) appear to be in excellent homeostasis until one considers that nearly all of that oxygen is utilized for oxidative

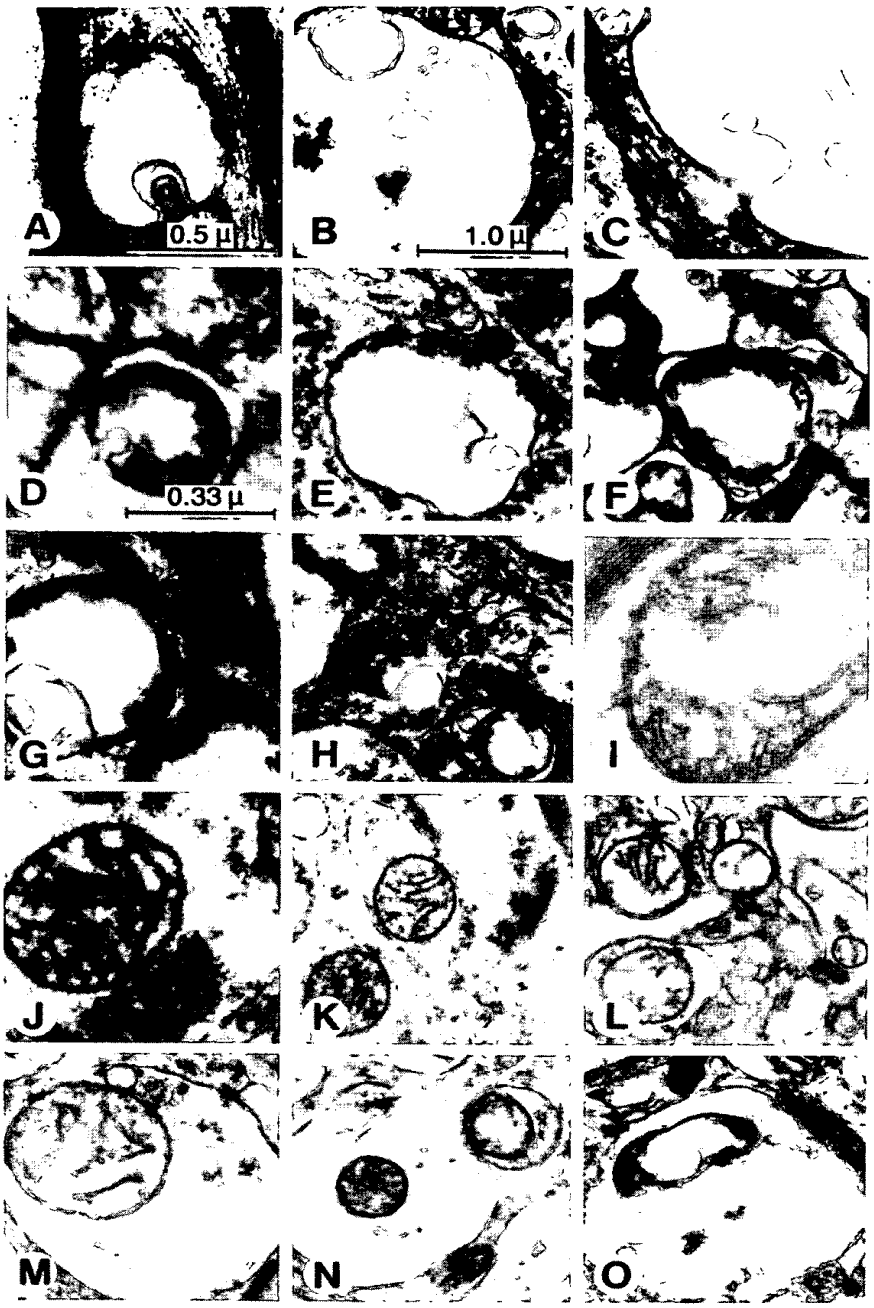

FIGURE 5. Gas microbubbles and their interactions with mitochondria. ×24,900 B, C, E, F, H, K–O; ×48,000 A, G, J; ×78,000, D, I. (A) Ethyl ether (2G, WM); gas bubbles forming within gas bubbles. (B) Ethyl ether (2G, WM); gas bubbles entrapped within gas bubbles. (C) Ethyl ether (2G, WM); gas bubbles entrapped within gas bubbles. (D) Halothane (2G, GM); gas bubble entering a mitochondrion. (E) Control (2G, GM); oxygen (likely) bubble entering a swollen mitochondrion. (F) Halothane (3G, GM); gas bubble entering a mitochondrion. (G) Ethyl ether (2G, GM); gas bubble in a swollen mitochondrion. (H) Methoxyflurane (2G, GM); gas bubble in a swollen mitochondrion. (I) Enflurane (3G, WM); gas bubble in a swollen mitochondrion. (J) Flurothyl (3G, WM); somewhat swollen mitochondrion. (K) Pentane (3G, WM); swollen mitochondria. (L) Halothane (2G, GM); swollen mitochondria. (M) Isoflurane (3G, GM); swollen mitochondrion in a gas bubble. (N) Nitrous oxide (2G, GM); unswollen mitochondrion in a gas bubble. (O) Methoxyflurane (2G, GM); swollen mitochondrion in a gas bubble. 2G, 2% glutaraldehyde; 3G, 3% glutaraldehyde; GM, gray matter; WM, white matter. μ, μm (micron) ×24,900 (1.0), ×48,000 (0.5), ×78,000 (0.33).

metabolism within the mitochondria. Even if intramitochondrial water were generously estimated to be 1% of total brain water, mitochondrial water would have to turn over about 100 times per minute just to keep up with resting oxygen delivery. Such as oxygen delivery mechanism would be untenable, but if oxygen could be delivered or accumulate as gas bubbles within the mitochondria, its low water solubility would not limit its availability for aerobic metabolism. In Figure 4, the intramitochondrial gas could be oxygen, taken up but not utilized because of postmortem substrate limitations, or it could be nitrogen, carbon dioxide, or some mixture of the three gases.

Conclusions

Oxygen delivery from capillaries to mitochondria may be entirely in the form of transparent gas microbubbles. Partially swollen mitochondria probably represent normal histological configurations containing gases, principally oxygen, but also perhaps nitrogen, carbon dioxide or both.

GAS MICROBUBBLES IN ANESTHESIA

Results

In the most extensive portion of this pilot study, gas microbubbles are newly proposed as a mechanism by which inhalation anesthetics exert their pharmacological effects. The pictures of transparent gas bubbles in the brains of anesthetized perfused rats support their presence during anesthesia (Figures 1 and 3). Bubbles counted in the ×6000 pictures were tabulated for 20 anesthetized and 4 unanesthetized rats in Table 1. Limited sample sizes precluded meaningful statistical comparisons among anesthetics. However, that more bubbles were present in the brains of anesthetized rats than in those of the controls was generally supportable at a $p < .05$ level. In Figure 5, pictures with higher magnification provide evidence that the bubbles were gaseous, that is, transparent bubbles within bubbles (Figure 5A through C). Evidence for bubble targeting in Figure 5 includes bubbles entering mitochondria (Figure 5D through F); bubbles within mitochondria (Figure 5G through I); transparent, gas-filled mitochondria (Figure 5J through L); and mitochondria engulfed within gas bubbles (Figure 5M through O). Figure 6E through L shows bubble targeting for synaptic vesicles, many suspended in a gas phase; Figure 6M shows a gasfree vesicle field (nitrous oxide); Figure 6N shows totally gas-engulfed vesicles (ethyl ether); and Figure 6O (halothane) shows a nerve ending and synapse in a gas phase. Conversely, vesicles from the flurothyl rat (Figure 6A through D) appear to be damaged and may be prone to releasing neurotransmitters. Counter to the numerous gas bubbles in anesthetized rats perfused

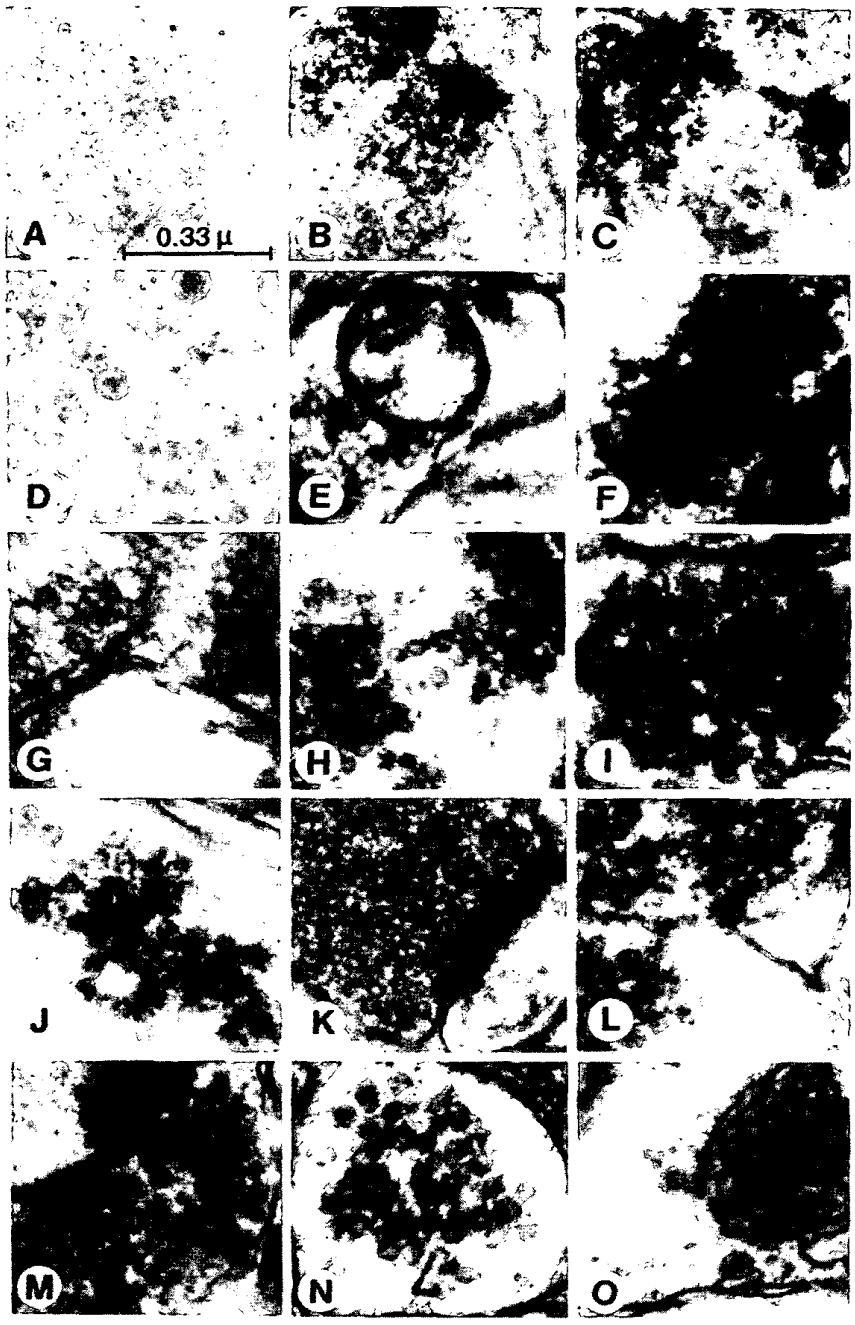

FIGURE 6. Synaptic vesicles entrapped in a gas phase. ×78,000. (A) Flurothyl (3G, WM), disrupted synaptic vesicles. (B) Flurothyl (3G, GM), disrupted synaptic vesicles. (C) Flurothyl (3G, GM), disrupted synaptic vesicles. (D) Flurothyl (3G, WM), small oval transparencies suggestive of angstromsized gas bubbles. (E) Halothane (2G, GM), synaptic vesicles, swollen mitochondrion. (F) Methoxyflurane (2G, WM), dense synaptic vesicles. (G) Halothane (2G, WM), synaptic vesicles in a gas phase. (H) Methoxyflurane (2G, WM), synaptic vesicles in a gas phase. (I) Ethyl ether (2G, GM), synaptic vesicles in a gas phase. (J) Nitrous oxide (2G, GM), synaptic vesicles in a gas phase. (K) Enflurane (3G, GM), vesicles at synapse with adjacent gas phase. (L) Xenon (3G, WM), synaptic vesicles in a gas phase. (M) Nitrous oxide (2G, GM), synaptic vesicles not in a gas phase. (N) Ethyl ether (2G, GM), synaptic vesicles totally engulfed in a gas phase. (O) Halothane (2G, WM), nerve ending, vesicles, and synapse in a gas phase. 2G, 2% glutaraldehyde; 3G, 3% glutaraldehyde; GM, gray matter; WM, white matter. μ, μm (micron).

with 2G or 3G, bubble numbers were dramatically reduced in 4 ether-anesthetized rats perfused with 7 to 50 mL of the 7.47× hypertonic buffered fixative (Figure 1, Table 1). Comparison of the numbers of bubbles counted in the cerebral cortex gray and white matter of ether-anesthetized rats perfused with 7 mL of 2G and 7 mL of the BF clearly shows that the BF depletes tissue gas microbubbles, $p < .001$.

Discussion

Since the first clinical use of ethyl ether and nitrous oxide as general anesthetics in the 1840s, several hypotheses have been published concerning anesthetic mechanisms (Paton 1984), most proposing a lipid site of action in keeping with the long-established Meyer-Overton rule, which links the potency of an anesthetic to its fat solubility. To date, no study has considered whether or not all the inhalation anesthetics might act in the same physical state—solid, liquid, or gas. Obviously, they cannot act as solids; neither could all inhalation anesthetics act in the form of liquids, because several agents, such as xenon, nitrous, oxide, and cyclopropane, are obligate gases at body temperature (see Boiling Points in Table 3). However, since vapor-pressure physics requires all volatile anesthetics to equilibrate into liquid *and* gas phases in vivo at body temperature (Rogers and Hill 1978), the author conceived the hypothesis that inhalation anesthetics may act in the form of gas microbubbles.

The actual presence of gas bubbles was demonstrated in the images in Figure 3 and Figure 5A through C, and more microbubbles were counted in the brains of anesthetized than for unanesthetized rats (Table 1). That anesthesia might result from the presence of gas bubbles was suggested by pictures of bubbles interacting with mitochondria and synaptic vesicles (Figures 5 and 6). In this mode, anesthetic gas bubbles are seen primarily as inert blocking agents—that is, they block the access of oxygen to the interior of mitochondria and block the release of neurotransmitters from synaptic vesicles. Because oxygen and/or nitrogen bubbles were present in the brains of control rats, their presence would be expected in the brains of anesthetized rats as well. Therefore, one could not assign a specific size range for activity of the anesthetic gas bubbles, but it appears that bubble size may correlate with anesthetic efficacy. Ultrasmall gas bubbles expected from the convulsant anesthetic flurothyl may surround or disrupt the membranes of 30- to 70-Å synaptic vesicles to effect a release of neurotransmitters. Somewhat larger (roughly 0.2 to 4.0 μm) bubbles, prevalent in the clinically effective volatile anesthetics, may merely surround synaptic vesicles to block neurotransmitter release. If these gas bubbles surround synaptic vesicles, they would also be expected initially to block transmitter reuptake. This fits conceptually with the early excitement phase of anesthesia commonly observed

prior to the advent of anesthetic premedication regimens. Microbubbles in the range of 0.2 to 4.0 μm could also surround and fill mitochondria to block oxygen uptake and thereby inhibit oxidative metabolism. It should be noted that this mechanism would not require depressed tissue levels of oxygen. The anesthetic competitive blockade could be effective in the presence of normal or even elevated levels of oxygen in brain tissue.

The larger gas bubbles seen in the less potent gas anesthetics nitrous oxide and xenon make them less effective at targeting synaptic vesicles and mitochondria; for example, nitrous oxide bubbles (Figures 3C and 5N) most often surround, but do not fill or cause swelling of mitochondria. Additional compelling evidence in support of a gas bubble mechanism for inhalation anesthesia is that it allows for plausible answers to the following enigmas noted by Koblin (1990):

(1) Why against the Meyer-Overton rule, is pentane an anesthetic, but the more fat-soluble alkanes, octane and decane, are inactive?

Probable answer: pentane boils at 36.1°C and is therefore a gas at body temperature. It was shown to be a weak anesthetic when 50 mL was added to the anesthetic chamber (Table 1). Identical volumes of octane and decane were inactive, as might be expected, because their high boiling points (see Table 3) would predict very low vapor pressures at body temperature.

(2) Why is isoflurane nearly one and a half times more potent than its chemical isomer, enflurane?

Probable answer: again, vapor pressure; the boiling point of isoflurane (48.5°C) is lower and its vapor pressure higher than that of enflurane (56.5°C), making it more bioavailable as gas microbubbles in vivo for equal volumes of vaporized liquid (see Table 3).

(3) Why does flurothyl possess major convulsant potential?

Probable answer: flurothyl may target synaptic vesicles to effect a release of neurotransmitters. The flurothyl rat (Table 1) convulsed for 4 min prior to the onset of anesthesia. With a boiling point of 63.9°C, flurothyl would exhibit a vapor pressure similar to that of chloroform and would equilibrate into gas and liquid phases in the brain. Perfluoronation of its terminal carbon atoms may confer flurothyl with extreme hydrophobicity and thus favor the formation of angstrom-sized bubbles, which physically target synaptic vesicles. Indoklon (flurothyl) has been used to evoke convulsions in humans as a substitute for electroconvulsive therapy (Small and Small 1972). With an effective dose of only 0.25 mL

of vaporized liquid, only a few μL of flurothyl could be present per g of brain tissue, which is consistent with targets that have small synaptic vesicles. As well, its high fat solubility may favor interactions with synaptic vesicle membranes.

Hydrophobicity (fat solubility) appears to provide a structure-activity relationship in volatile anesthetics. Compound 485 (Koblin et al. 1981) is a more volatile isomer of enflurane and isoflurane and would therefore be expected to be the most potent of the three. Instead, it is a convulsant anesthetic. Like flurothyl, compound 485 exhibits complete hydrophobic halogenation of its terminal carbon atoms, a structural feature shared by several convulsant anesthetics (Rudo and Krantz 1974). Therefore, volatility is a required, but not a sufficient, attribute for utility as an inhalation anesthetic.

Water solubility may dictate the spectrum of gas bubble sizes which, in turn, may be the primary determinant of the physical targeting of the agent. This hypothesis demands that volatile anesthetics equilibrate in vivo between liquid and gas phases, in keeping with the vapor-pressure curves reported by Rogers and Hill (1978). In support of this, the in vivo nuclear magnetic resonance fluorine signal from halothane in anesthetized rats and rabbits was reported as having short (3.5 ms) T2 values ranging up to 43 ms (Evers et al. 1987) and to 65 ms (James et al. 1987). Whereas the short T2 values probably represent halothane in the liquid state, longer T2 values could reflect slowed spin-spin relaxation rates of microbubbles of halothane in the gaseous state. Interestingly, Evers and colleagues (1987) described those halothane signals as arising from two differing compartments.

Conclusions

Evidence points to the probability that gas and volatile anesthetics may act in the form of gas microbubbles and that the anesthetic targets may include synaptic vesicles and mitochondria. Important attributes required for activity as a volatile anesthetic are a boiling point that provides for a significant vapor pressure at body temperature and a level of hydrophobicity that favors the formation of gas bubbles, generally ranging from 0.2 to 4.0 μm in diameter.

GENERAL DISCUSSION AND CONCLUSIONS

The statistical data in Table 1 were included only to suggest trends in the data. The exception would be comparisons between the ether-anesthetized rats perfused with 2G and BF. Here, the data clearly

support the observation that fixation with BF causes the loss of tissue bubbles ($p < .001$), presumably secondary to the loss of extracellular and intracellular fluid. Clearly, the most important finding of this study is the observation of the gas microbubbles per se, and the importance of the tonicity of the fixative solution in displaying these bubbles. Because the current use of hypertonic fixation fluids may be commonplace, one might ask, Why has this practice developed? The normal presence of gas microbubbles in tissues may create so much noise after isotonic fixation that intracellular detail becomes obscure. Certainly, one can appreciate much more tissue detail in Figure 1B than in Figure 1A. Would you paint a picture of a barn in sunlight or in a snowstorm? Hypertonic fixation gets rid of the snow (gas microbubbles)! However, as useful as these hypertonic fixation procedures have proven for assessment of minute structural detail, their widespread acceptance has long delayed studies on the presence and importance of gas microbubbles in tissue.

The use of physiological, near-isotonic fixative solutions has led to the identification of a new microcompartment in the body. This compartment, consisting of gas microbubbles, appears to play significant roles in physiology (oxygen transport), toxicology (CCl_4-induced hepatotoxicity), and pharmacology (inhalation anesthesia). Evidence suggests that some anesthetic gas microbubbles may physically block oxygen uptake into mitochondria, whereas others have releasing or reuptake blocking effects on synaptic vesicles. Targeting of membrane-limited organelles such as mitochondria and synaptic vesicles may constitute the primary mechanism of the pharmacological and toxicological actions of these gas microbubbles. Electron microscopy coupled with isotonic tissue fixation should provide a new tool for research in the biological sciences.

REFERENCES

Evers, A. S., Berkowitz, B. A., and d' Avignon, D. A. 1987. Correlation between the anesthetic effect of halothane and saturable binding in the brain. *Nature* 328:157–160.

deFerreyra, E. C., Villarreul, M. C., Fernandez, G., deFenos, O. M., Bernacchi, A. S., deCastro, C. R., and Castro, J. A. 1989. Further studies on the mechanism of the late protective effects of phenylmethylsulfonylfluoride on carbon tetrachloride–induced liver necrosis. *Exp. Mol. Pathol.* 50:253–269.

Gonzales-Aguilar, F. 1969. Extracellular space in the rat brain after fixation with 12M formaldehyde. *J. Ultrastructure Res.* 29:76–85.

Goodman and Gilman. 1990. *The Pharmacologic Basis of Therapeutics*, Eighth Edition, 286. Elmsford, NY: Pergamon Press.

James, T. L., Chang, L.-H., Chew, W., Gonzalez-Mendez, R., Litt, L., Mills, P., Moseley, M., Pereira, B., Sessler, D., and Weinstein, P. R. 1987. In situ brain metabolism. *Ann. N. Y. Acad. Sci.* 508:64–78.

Koblin, D. D. 1990. Mechanism of Action. In *Anesthesia,* ed. R. D. Miller, 51–83. New York: Churchill Livingstone.

Koblin, D. D., Eger, E. I. III, Johnson, B. H., Collins, P., Harper, M. H., Terrell, R. C., and Speers, L. 1981. Minimum alveolar concentrations and oil/gas partition coefficients of four anesthetic isomers. *Anesthesiology* 54:314–317.

Larson, R. E., and Plaa, G. L. 1965. A correlation of the effects of cervical cordotomy, hypothermia, and catecholamines on carbon tetrachloride–induced hepatic necrosis. *J. Pharm. Exp. Ther.* 147:103–111.

Marzi, A., deToranzo, E. G. D., and Castro, J. A. 1980. Mechanism of chlorpromazine prevention of carbon tetrachloride–induced liver necrosis. *Toxicol. Appl. Pharmacol.* 52:82–88.

Merck Index, Twelfth Edition, 1996. Whitehouse Station, NJ: Merck Research Laboratories, Merck & Co., Inc.

Oberling, C., and Rouiller, C. 1956. Les effects de l'intoxication aigue au tetrachlorure de carbone sur le foie du rat: étude au microscope électronique. *Ann. Anat. Pathol.* 1:401–427.

Paton, W. D. M. 1984. How do we understand anaesthesia? *Eur. J. Anaesthiol.* 1:93–103.

Rogers, R. C., and Hill, G. E. 1978. Equations for vapor pressure versus temperature: derivation and use of the Antoine equation on a hand-held programmable calculator. *Br. J. Anaesth.* 50:415–424.

Rudo, F. G., and Krantz, J. C. Jr. 1974. Anesthetic molecules. *Br. J. Anaesth.* 46:181–189.

Small, J. G., and Small, I. F. 1972. Clinical results: indoklon versus ECT. *Semim. Psychiatry* 4:13–26.

Sumi, S. M. 1969. The extracellular space in the developing rat brain: its variation with changes in osmolality of the fixative, method of fixation, and maturation. *J. Ultrastructure Res.* 29:76–85.

Villarreul, M. C., Fernandez, G., deFerreyra, E. C., deFenos, O. M., and Castro, J. A. 1986. Late preventive effects of trifluoperazine on carbon tetrachloride–induced hepatic necrosis. *Toxicol. Appl. Pharmacol.* 83:287–293.